E × B shear suppression of turbulence in diverted H-mode plasmas; role of edge magnetic shear

T.S. Hahm[1], D.H. Na[1], J.W. Lee[1], J.W. Park[1], and Y.S.Na[1]
S.S. Kim[2], W.H. Ko[2], P.H. Diamond[2, 3], Hogun Jhang[2], and Y.M. Jeon[2]

[1]Department of Nuclear Engineering, Seoul National University, Seoul 151-744, Korea
[2]National Fusion Research Institute, Daejeon 305-806, Korea
[3]*CASS and CMTFO, University of California at San Diego, California 92093, USA*

Corresponding authour : tshahm@snu.ac.kr

Abstracts. We show that strong edge magnetic shear which is generic to divertor plasmas makes the E × B shearing of turbulence eddys in toroidal geometry more effective. From calculations of the E × B shearing rates for KSTAR edge parameters, we conclude that the enhanced magnetic shear at the diverted KSTAR plasma edge facilitates E × B shear suppression of turbulence and ensuing H-mode transition.

1. Introduction

Physical understanding of H-mode transition is an urgent issue in providing a predictive capability for successful operation of ITER. It is widely accepted that the transition and transport reduction are closely related to the E × B flow shear which develops just inside the LCFS(last closed flux surface) [1]. In addition, a beneficial effect of a diverted plasma for an easier transition has been known since the discovery of the H-mode [2]. Some tokamaks without divertors have never achieved H-mode plasmas and the power threshold for limiter plasmas is higher than that for diverted plasmas. While this difference has been attributed to the fact that higher SOL(scrape off layer) transparency for neutrals in limiter plasmas leads to larger convective energy loss in [3], we focus on the effects from stronger edge magnetic shear in divertor plasmas in this paper. This approach is supported by an H-mode transition of a limiter plasma which is induced by current ramp down [4]. That work [4] also acknowledges an importance of enhanced edge magnetic shear produced by the current ramp down.

KSTAR tokamak has achieved H-mode plasmas well ahead of its original schedule [5]. An interesting feature of KSTAR plasmas at the H-mode transition is an abrupt increase in its edge q value and elongation [6]. Often, this happens as the plasma becomes diverted losing a contact with the outer limiter. Motivated by the KSTAR results, we investigate how plasma boundary shape such as x-point and elongation modifies the E × B shearing rate and microturbulence at the edge in this work.

In this work, we show that strong edge magnetic shear which is generic to divertor plasmas changes the radial structure of the E × B shearing rate [7, 8] in toroidal geometry and makes the radial decorrelation of edge turbulence [9] more effective. This possibility has been discussed in [8]. This work contains more quantitative analyses and explicit examples from KSTAR plasmas. Consequently, we conclude that the E × B shear suppression of turbulence [10] which is widely regarded as the common H-mode transition mechanism [1, 9] works more effectively in diverted plasma edge.

The rest of this paper is organized as follows; In Sec. 2, we adopt a simple analytic model [11] for a diverted plasma, and demonstrate that a logarithmic divergence of the flux surface averaged q_{MHD} and a stronger algebraic divergence of magnetic shear $\hat{s}$ near the LCFS. In Sec.

3, we investigate contribution of the magnetic shear to the E × B shearing rate in toroidal geometry [8]. In Sec. 4, the E × B shearing rate has been evaluated at KSTAR pedestal region, using the CES(Charge Exchange recombination Spectroscopy) measured u_ϕ and T_i profiles at pedestal [12], a model pedestal density profile (in the absence of density profile data), neoclassical u_θ and the radial force balance relation. The resulting value is comparable to those from DIII-D H-mode [1] and C-Mod EDA H-mode [13]. A conclusion is drawn in Sec. 5.

2. Model diverted plasma configuration

In the simple analytic model for a diverted plasma [11], the poloidal flux function is given by;

$$\psi = \frac{R_0 B_\phi}{2L_q}\left(x^2 - \frac{a^2}{2}\cos\left(\frac{\pi y}{\kappa a}\right)\right) \quad (1)$$

where (x, y) is the Cartesian coordinate, a is minor radius, κ is elongation at the LCFS. Note that the elongation at the axis becomes $\frac{2\kappa}{\pi}$ according to this model. Since $\vec{B} = B_\phi R\vec{\nabla}\zeta + \vec{\nabla}\zeta \text{ x } \vec{\nabla}\psi$, the poloidal magnetic field is given by

$$B_\theta^2 = B_\emptyset^2\left\{\left(\frac{x}{L_q}\right)^2 + \left(\frac{\pi a}{4\kappa L_q}\right)^2 \sin^2\left(\frac{\pi y}{\kappa a}\right)\right\}. \quad (2)$$

This vanishes at the x-points, $(0, \kappa a)$ and $(0, -\kappa a)$. The corresponding q_{MHD} can be obtained from

$$q_{MHD} \cong \frac{B_\emptyset}{2\pi R_0}\oint \frac{dl}{B_\theta} = \frac{4}{\pi^2}\kappa q_c K(\rho)\ , \quad (3)$$

where $q_c \equiv L_q/R_0$ is the reference value of the safety factor for circular flux equilibrium, $K(\rho)$ is the complete elliptic integral of first kind, $\rho \equiv x/a$ is the normalized radial coordinate (ρ = 1 at the separatrix, ρ = 0 at the axis). This exhibits a logarithmic divergence of q_{MHD} near the separatrix. The corresponding magnetic shear is given by $\hat{s} \equiv \frac{d\ln q_{MHD}}{d\ln\rho}$ which shows a stronger algebraic divergence near the separatrix [11].

3. Magnetic shear dependence of the E × B shearing rate

The E × B shearing rate [7] for an isotropic turbulent eddy $L_r \cong L_\theta$ in a shaped plasma is given by $\omega_{E\times B} = \frac{(RB_\theta)^2}{B}\frac{\partial}{\partial\psi}\left(\frac{E_r}{RB_\theta}\right)$. While this quantity can be evaluated for a specific plasma, given a set of experimental values of E_r, B_θ, etc, we can characterize the potentially beneficial effects of magnetic shear, safety factor, and elongation by adopting a simpler high aspect ratio version [8] of the E × B shearing rate given by $\omega_{E\times B}^{(0)} = \frac{r}{q}\frac{\partial}{\partial r}\left(\frac{qE_r}{rB}\right)$, and a simple double-null analytic model described in Sec 2. more easily.

By separating the contribution from E_r shear from that of magnetic shear, we obtain

$$\omega^{(0)}_{E\times B} = \frac{r}{q}\frac{\partial}{\partial r}\left(\frac{qE_r}{rB}\right) = r\frac{\partial}{\partial r}\left(\frac{E_r}{rB}\right) + \frac{E_r}{B}\frac{1}{q}\frac{\partial q}{\partial r} = \omega^{BDT} + \frac{E_r}{rB}\hat{s} \quad (4)$$

Here, ω^{BDT} is the cylindrical expression from Ref. [10], the last term is a contribution from the magnetic shear. While one would usually expect that the last term is subdominant to the ω^{BDT} from the E_r shear at the H-mode pedestal, there are examples from ITB (internal transport barrier) plasmas in which the contribution from B_θ variation to the Hahm-Burrell shearing rate, $\omega_{E\times B}$ [7] is significant [14-16]. Since $\hat{s}$ diverges at the LCFS, we expect that the last term's contribution can be significant near the LCFS of diverted plasmas.

Recent Doppler backscattering measurements on DIII-D show that prior to the H-mode transition and at the early phase of H-mode, the E × B shear becomes highest at the narrow outboard E_r-well, before it broadens inward in the later phase of H-mode [17]. This suggests the importance of E_r shear dynamics near LCFS at the H-mode transition. Furthermore, an important role of the turbulence driven zonal flows in the pre-transition limit cycle oscillation phase as captured in a simple one-dimensional predator-prey model [18] has been emphasized. We note that the proper E × B shearing rate of the time-dependent zonal flows [19] also includes the magnetic shear dependence discussed in this paper, while limited diagnostics capabilities at present time do not allow meaningful assessment of a possible role of zonal flows in KSTAR H-mode transition. The value of E_r at the LCFS is determined by many factors. In the SOL outside the LCFS, the electron loss along the magnetic fields to the divertor plate should dominate to make E_r positive, while inside the LCFS, the perpendicular dynamics should be dominant in determining the E_r structure. Typical E_r profiles in the H-mode pedestal region from various tokamaks exhibit a well structure [1].

As a consequence, ω^{BDT} which is proportional to $\frac{\partial}{\partial r}\left(\frac{E_r}{rB}\right)$, changes its sign from negative to positive across the bottom of the E_r-well. While overall magnitude of ω^{BDT} is large enough to justify suppression of turbulence in the pedestal region, ω^{BDT} vanishes at the bottom of E_r-well which roughly corresponds to the middle of pressure pedestal. Therefore, locally there is no beneficial effect of the E × B shearing. Furthermore, while the curvature of E_r is significant at that point, there's no mode-independent generic effect of radial decorrelation due to the E_r curvature [20], unlike the effect from E × B shear. However, mode-specific effect, in particular for the dissipative trapped electron mode [21], exists.

On the other hand, the E × B shearing rate for a high aspect ratio tokamak [8] is proportional to $\frac{\partial}{\partial r}\left(\frac{qE_r}{rB}\right)$ as shown in Eq. (4). For limiter plasmas in which radial variation of q at the edge is not sharp, the radial variation of E_r mostly determines the magnitude and shape of the E × B shearing rate in toroidal geometry. However for diverted plasmas, both q and $\hat{s}$ diverge toward the LCFS. Unlike the profile of E_r, $\frac{qE_r}{rB}$ decreases monotonically in radius at the diverted H-mode plasma edge. Therefore, the toroidal version of the E × B shearing rate $\omega^{(0)}_{E\times B}$ tends to have the same sign across the H-mode plasma pedestal region. This observation illustrates that the second term of Eq. (4) which depends on the magnetic shear explicitly, has a significant effect on the overall profile of $\omega^{(0)}_{E\times B}$. A specific example of these features from KSTAR H-mode plasmas is shown in the next section.

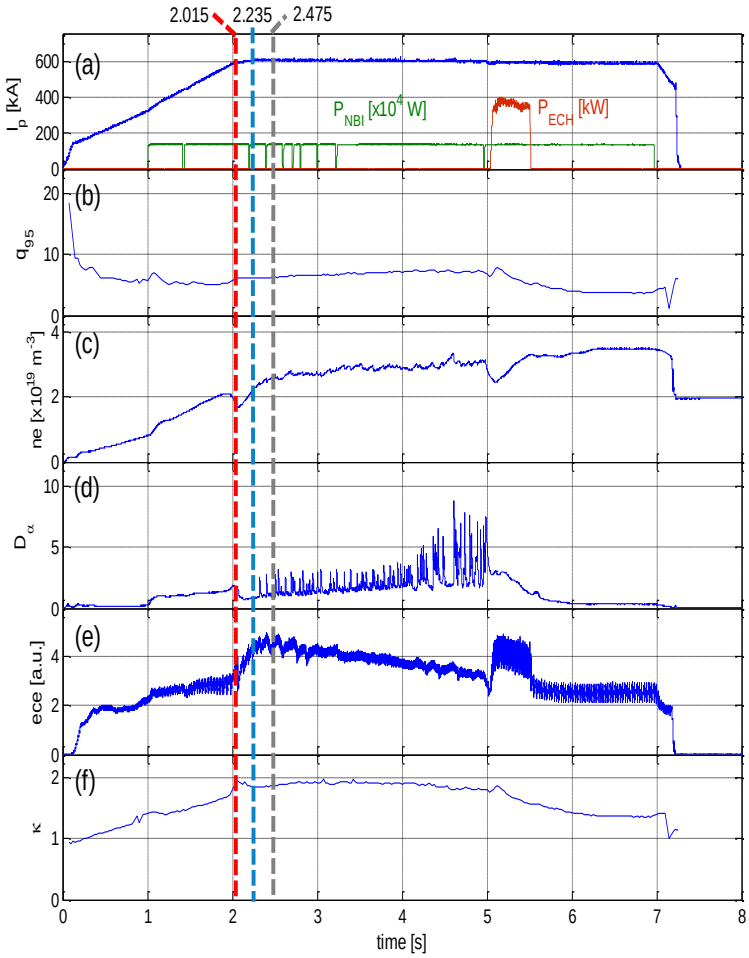

Figure 1 *Time trace of plasma parameters of KSTAR shot #5680, (a) plasma current and auxiliary power, (b)* $\boldsymbol{q_{95}}$*, (c) line averaged electron density, (d)* $\boldsymbol{D_\alpha}$*, (e) electron temperature measured by ECE, (f) plasma elongation,* $\boldsymbol{\kappa}$

4. Validation with KSTAR experimental results

We have estimated the E × B shearing rate for the KSTAR plasma shot # 5680 around the H-mode transition time. At this time, the heating rate was held constant with no resonant magnetic perturbation (RMP) imposed. Co-current neutral beam injection (co-NBI) was held at 1.5 MW from 1 sec to 6.9 sec. On the other hand, x-point was formed completely as the plasma got detached and diverted. Fig. 1 exhibits time evolutions of plasma current, q_{95}, line-integrated density, D_α signal, ECE signal, and plasma elongation, respectively.

Note that plasma was in the L-mode state at t = 2.015 sec, while t = 2.235 sec and t = 2.475 were after the H-mode transition. For an estimation of the E × B shearing rate, informations on E_r, B_θ, and B_ϕ are required. In the absence of E_r measurements from KSTAR experiment, we use the radial force balance,

$$E_r = \frac{1}{n_i e Z_i}\frac{\partial}{\partial r}P_i - u_\theta B_\phi + u_\phi B_\theta \qquad (5)$$

For an estimation of E_r, we need to know u_ϕ, u_θ, B_ϕ, B_θ as well as n_I and T_I. We use the measured values of u_ϕ and T_i. B_θ and B_ϕ can be estimated using the EFIT code [22]. u_θ can be calculated from the neoclassical theory [23]. However, we need to make a model density profile in the absence of profiles from measurements. Here a tangent hyperbolic function is used for a fitting (solid line) as described in Appendix A. Normalized poloidal magnetic flux function, ψ_N calculated using the EFIT is shown in Fig. 2. Here, $\psi_N = (\psi - \psi_0)/(\psi_a - \psi_0)$ (where ψ_0: poloidal magnetic flux at magnetic axis, ψ_a: poloidal magnetic flux at separatrix) . Formation of a diverted plasma is apparent. Ion temperature profile at t = 2.235 sec is shown in Fig. 3 as a function of ψ_N. u_ϕ profile at t = 2.235 sec is shown in Fig. 4 where a smoothed cubic spline fitting was used for the solid line. Fig. 5 and Fig. 6 show T_i profiles and u_ϕ profiles at t = 2.015 sec (L-mode), t = 2.235 (right after H-mode transition), and t = 2.475 (well into H-mode) respectively. Both manifest the formation of a pedestal after the H-mode transition.

Construction of a model density profile requires a few assumptions since only the line-averaged $\bar{n}_e$ was available for this plasma. We describe this procedure in the Appendix A. The model n_e- profiles at t = 2.015 sec, t = 2.235 sec, and t = 2.475 sec are shown in Fig. 7. For u_θ, we use the formulas from the Hirshman-Sigmar moment approach [24]. This is presented in the Appendix B. From these considerations, we calculated three terms on the RHS of Eq. (5). Finally, we can calculate E_r and the E × B shearing rate. Contributions of each term on the RHS and the resulting E_r at t = 2.235 sec are plotted in Fig. 8. This indicates the dominant contribution from the $\frac{\partial P_i}{\partial r}$ term after the H-mode transition. Also note that $E_r >$ 0 in the core due to the contribution from co-current direction u_ϕ. From this, we can calculate $\omega^{(0)}_{E\times B}$[8] and $\omega_{E\times B}$[7].

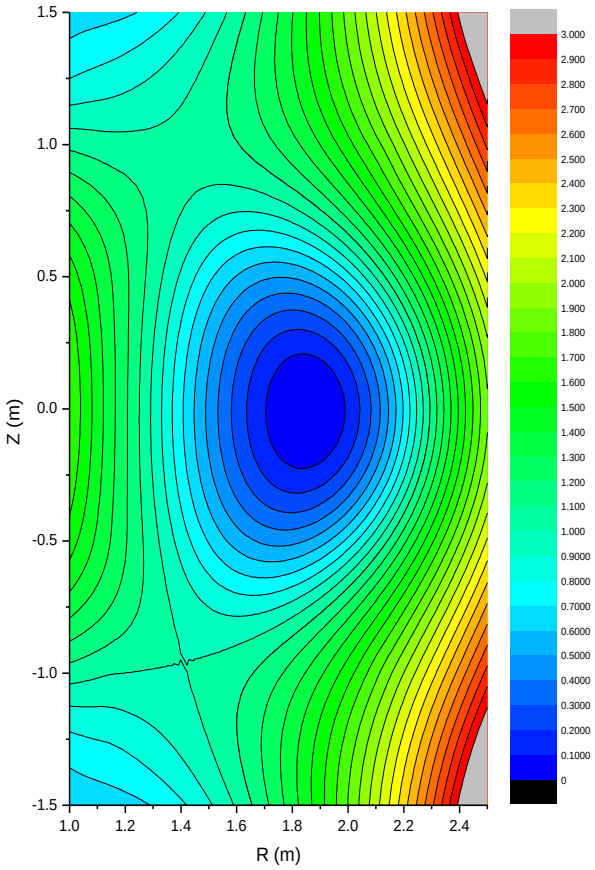

Figure 2 *Normalized poloidal magnetic flux function, $\boldsymbol{\psi_N}$ calculated using the EFIT at t=2.235 second of KSTAR shot #5680.*

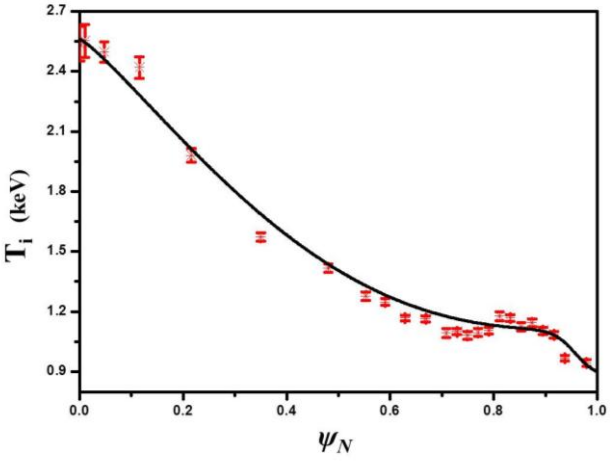

Figure 3 *Ion temperature profile measured by CES at t=2.235 second of KSTAR shot #5680.*

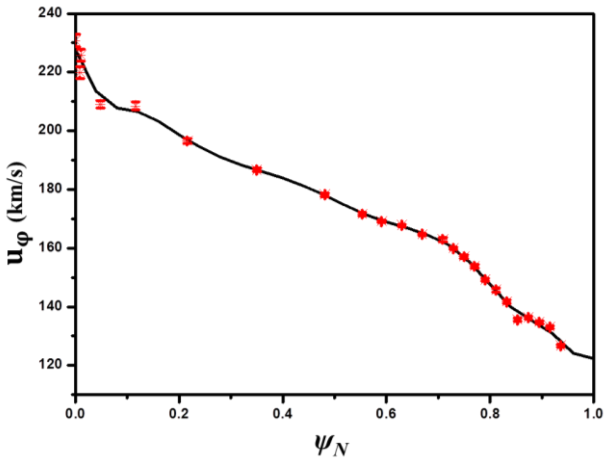

Figure 4 *Toroidal velocity profile measured by CES at t=2.235 second of KSTAR shot #5680.*

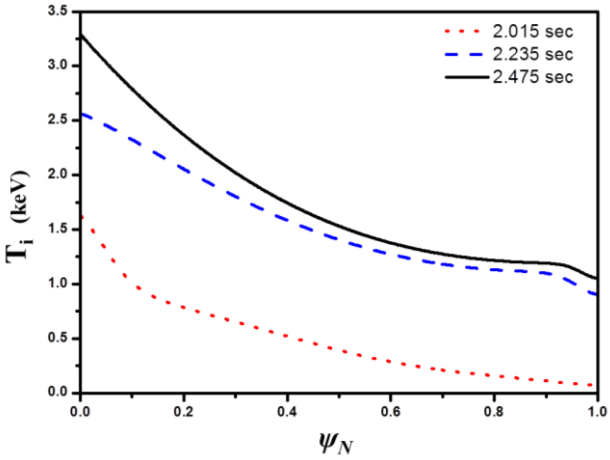

Figure 5 *Ion temperature profile at t=2.015 sec, 2.235 sec, and 2.475 sec of KSTAR shot #5680.*

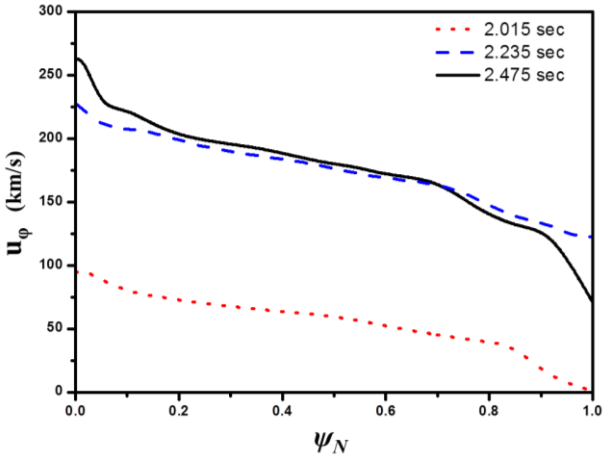

Figure 6 *Toroidal velocity profile at t=2.015 sec, 2.235 sec, and 2.475 sec of KSTAR shot #5680.*

As we have discussed in Sec. 3, ω^{BDT} in cylindrical geometry is proportional to $\frac{\partial}{\partial \mathrm{r}}\left(\frac{E_r}{rB}\right)$, and changes its sign from negative to positive across the bottom of the E_r-well in H-mode plasma edge as shown in Fig. 9. On the other hand, the E × B shearing rate for a high aspect ratio tokamak, $\omega^{(0)}_{E\times B}$[8] is proportional to $\frac{\partial}{\partial \mathrm{r}}\left(\frac{qE_r}{rB}\right)$.

For limiter plasmas in which the radial variation of q at the edge is not sharp, the radial variation of $\omega^{(0)}_{E\times B}$ is governed primarily by that of E_r. For instance, Fig. 10 shows a profile of $\frac{\mathrm{qE_r}}{rB}$ from the KSTAR plasma shot # 5680 at 2.235 sec using a model q profile with $q(a) = 7$ in blue. This shows a well structure such as that for E_r. However for diverted plasmas, both q and $\hat{s}$ diverge toward the LCFS. In this case, unlike the profile of E_r, $\frac{\mathrm{qE_r}}{rB}$ decreases monotonically in radius at the H-mode plasma edge. This is illustrated with a q profile with $q(a) = 12$ in black, from KSTAR plasma shot # 5680 at 2.235 sec. While q(r) should approach infinity as $\psi_N \to 1$ (r → a), a finite number of radial points used in EFIT calculation do not allow us to use $q(a) = \infty$. With this constraint, we use $q(a) = 12$ which nevertheless illustrates our main points. The corresponding $\omega^{(0)}_{E\times B}$ has the same sign across the H-mode plasma pedestal region as shown in Fig. 11. This shows the important role played by the strong magnetic shear represented by the second term on the RHS of Eq. (4).

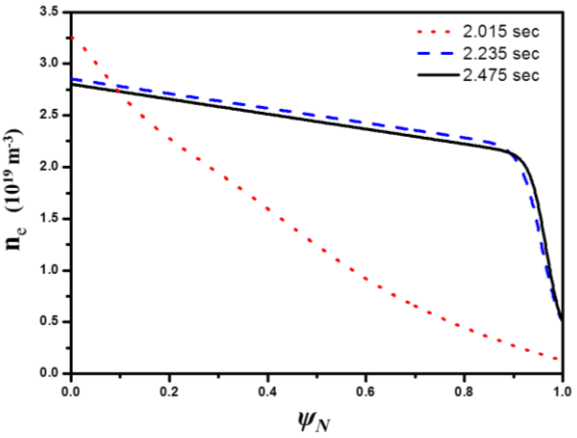

Figure 7 *The model of electron density profile at t=2.015 sec, 2.235 sec, and 2.475 sec of KSTAR shot #5680.*

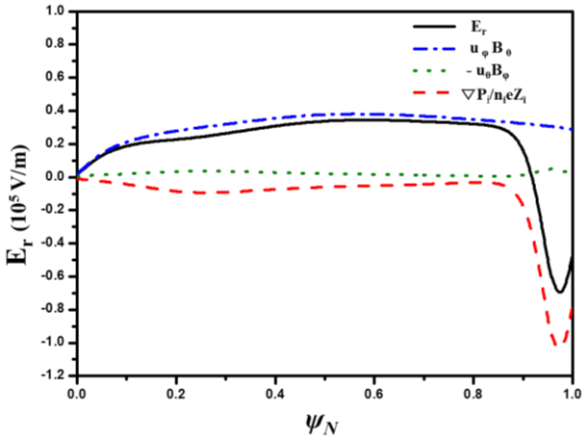

Figure 8 E_r *profile at t=2.235 second of KSTAR shot #5680.*

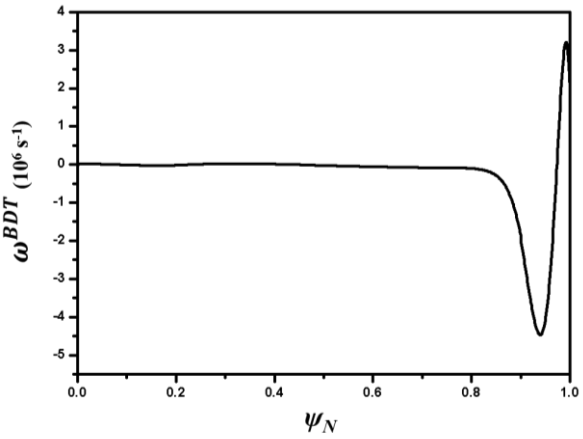

Figure 9 ω^{BDT} *profile at t=2.235 second of KSTAR shot #5680.*

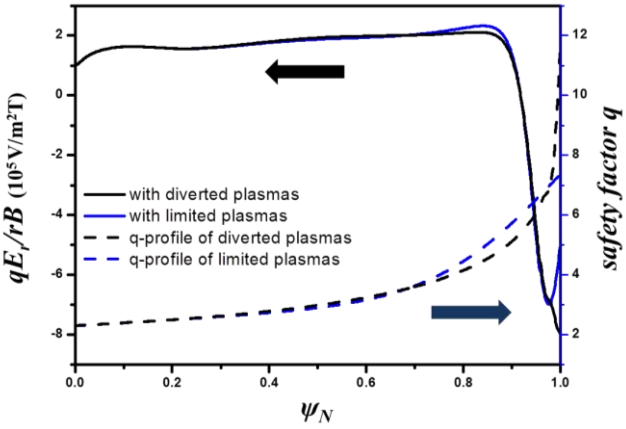

Figure 10 qE_r/rB *profile and* q *profile at t=2.235 second of KSTAR shot #5680.*

Since the density gradient of the first term in Eq. (5) is the dominant contributor to E_r in the H-mode pedestal as shown in Fig. 8, sensitivity of the E_r profile on the parameters used in the KSTAR density profile model should be kept in mind. In the absence of direct measurements of E_r or of n_e and u_θ from KSTAR to date, more quantitatively accurate illustration of radial structure of E_r and that of qE_r/rB seems unlikely. However, since the E_r-well is a robust feature of H-mode plasmas and KSTAR shares many commonalities with H-mode plasmas of other tokamaks [6], we expect that qE_r/rB monotonically decreases with its monotonically increasing absolute value in radius, while E_r profile has a local minimum just inside LCFS in KSTAR H-mode plasmas as well.

It has been shown that the variation of local magnetic shear on the same magnetic surface near LCFS can have a significant effect on tilting of turbulent eddys [25]. We expect that the variation of the E × B shearing rate on the same flux surface as characterized by Eq. (6) can have a similar significant effect on eddy tilting and the analyses based on this extension could bring more accurate condition for turbulence suppression. This is beyond the scope of this present study and will be addressed in the near future.

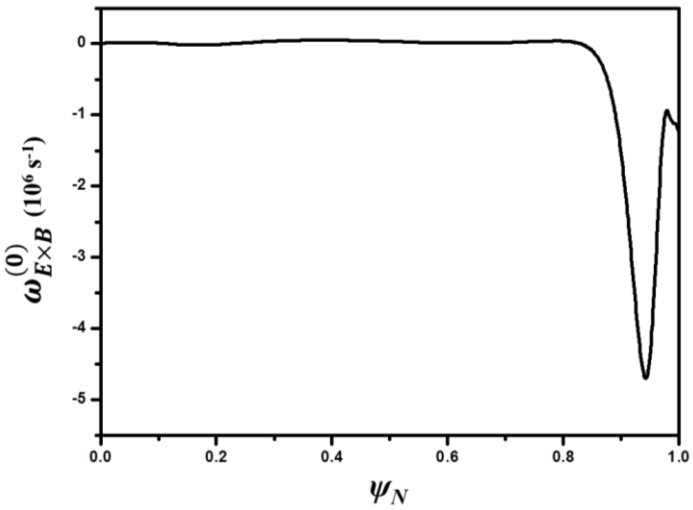

Figure 11 $\omega^{(0)}_{E\times B}$ *profile at t=2.235 second of KSTAR shot #5680 with* $\mathbf{q(a) = 12}$.

5. Conclusion

We have adopted a simple analytic model [11] for a diverted plasma, and demonstrated a logarithmic divergence of the flux surface averaged q_{MHD} and a stronger algebraic divergence of magnetic shear ŝ near the LCFS (last closed flux surface). We have also investigated contribution of the magnetic shear to the E × B shearing rate in toroidal geometry [8]. In comparison to the cylindrical expression [9] without explicit contributions from ŝ and q, the toroidal expression has an additional contribution from ŝ which tends to eliminate the null point of the E × B shearing rate just inside the LCFS of diverted plasmas at the H-mode transition.

In addition, the E × B shearing rate has been evaluated at KSTAR pedestal region, using the CES-measured u_ϕ and T_i profiles at pedestal, a model pedestal density profile (in the absence of density profile data), neoclassical u_θ and the radial force balance relation. In the pedestal region after the transition, the peak value of the general toroidal geometry shearing rate [8] was on the order of $10^6 sec^{-1}$, comparable to the value of the cylindrical shearing rate [10] from the DIII-D edge [1], and that of high aspect ratio shearing rate prediction [8] from the C-Mod EDA H-mode [13]. Of course, this fact alone does not elucidate the causality of H-mode transition. Due to limited measurements of profiles and fluctuations, from our analyses alone, we cannot rule out possible roles of various stabilizing mechanisms such as one discussed in [26] other than the E × B shear induced fluctuation suppression.

In conclusion, our studies support the working hypothesis that enhanced magnetic shear at diverted KSTAR plasmas facilitates the E × B shear suppression of turbulence and therefore makes the H-mode transition easier.

Acknowledgments

This research was supported by National R&D Program (NRF-2012M1A7A1A02-034893), and the International Research and Development Program (Grant No.2012-054738), the Korea Science and Engineering Foundation(KOSEF) grant (No. 2008-0062208) and by the World Class Institute (WCI) Program of the National Research Foundation of Korea(NRF) funded by the Ministry of Education, Science and Technology of Korea(MEST).

Appendix A : Construction of H-mode density profiles

We describe how electron density profile is reconstructed using the following assumptions.
1) The electron density profile of H-mode plasma can be approximated by the following tangent hyperbolic function.

$$f(x) = f_0 + a_{f_0}(\tanh[2(1 - x_{mid})/\Delta] - \tanh[2(\mathrm{x} - x_{mid})/\Delta]) + a_{f_1} H(1 - x/x_{mid})[1 - (x/x_{mid})^{\alpha_{f_1}}]^{\alpha_{f_2}} \quad \text{(A1)}$$

where a_{f_0}, a_{f_1}, a_{f_2} are constants. f_0, x_{mid} and Δ represent the value of $f(x)$ at the plasma boundary, the normalized poloidal flux function at the middle of pedestal, and the width of pedestal respectively.

2) The peakedness of KSTAR H-mode electron density profile is approximated by 1.3. [27]
3) The width of density pedestal is equal to the width of ion temperature pedestal.
4) The electron density from the axis (at core) to the pedestal top can be approximated by a line (linear function).
5) We match the value for line-averaged electron density of the reconstructed profile the measured one.
6) We take $n_e = 0.5 \times 10^{19}/m^3$ at the plasma boundary $\psi_N = 1$.

In addition, we assume

$$n_e(r) = n_{e0}[1 - (r/R_0)^2]^2 \quad \text{(A2)}$$

for the L-mode plasma. From these assumptions, we obtain the density profiles shown in Fig. 7 of the main text.

Appendix B : Model for ion poloidal flow

For ion poloidal flow velocity, we use the formulas from Hirshman and Sigmar moment approach [22].

$$u_\theta^i = \frac{1}{2} V_{T_i} \rho_i (K_1 \frac{1}{L_{T_i}}) \frac{B B_t}{\langle B^2 \rangle} \quad \text{(B1)}$$

where $L_{T_i}^{-1} \equiv dlnT_i/dr$, $v_{T_i} \equiv \sqrt{2T_i/m_i}$, $\rho_i \equiv m_i v_{T_i}/Z_i eB$.

$$K_1 \equiv D^{-1} \mu_{01}^i (\sqrt{2} + \alpha - \alpha\beta) \quad \text{(B2)}$$
$$D \equiv \mu_{00}^i \left(\mu_{11}^i + \sqrt{2} + \alpha - \alpha\beta\right) - \left(\mu_{01}^i\right)^2 \quad \text{(B3)}$$
$$\alpha \equiv n_I Z_I^2 / n_i Z_i^2 \quad \text{(B4)}$$
$$\beta \equiv \left(\frac{27}{4}\right)^2 \left(\frac{m_i}{m_I}\right)^2 \left(\frac{15}{2} + \sqrt{2\alpha} \frac{v_{T_i}}{v_{T_I}}\right)^{-1} \quad \text{(B5)}$$

Here, we assume $\alpha \equiv n_I Z_I^2 / n_i Z_i^2 \approx 0$, and take μ^is in the banana collisionality regime.

Reference

[1] Burrell K. H. 1997 Effects of E×B velocity shear and magnetic shear on turbulence and transport in magnetic confinement devices *Phys. Plasmas* 4 1499

[2] Wagner F. *et al* 1982 Regime of Improved Confinement and High Beta in Neutral-Beam-Heated Divertor Discharges of the ASDEX Tokamak *Phys. Rev. Lett* 49 1408-1412

[3] Kalupin D. *et al* 2006 Influence of the boundary conditions on the H-mode power threshold *Phys. Plasmas* 13 032504

[4] Toi K. *et al* 1990 Role of edge magnetic shear on the limiter H-mode transition of the JIPP T-IIU tokamak *Phys. Rev. Lett* 64 1895-1898

[5] Kwon M. *et al* 2011 Overview of KSTAR initial operation *Nucl. Fusion* 51 094006

[6] Yoon S.W. *et al* 2011 Characteristics of the first H-mode discharges in KSTAR *Nucl. Fusion* 51 113009.

[7] Hahm T. S., Burrell, K. H. 1995 Flow shear induced fluctuation suppression in finite aspect ratio shaped tokamak plasma *Phys. Plasmas* 2 1648

[8] Hahm T. S. 1994 Rotation shear induced fluctuation decorrelation in a toroidal plasma *Phys. Plasmas* 1 2940.

[9] Diamond P. H. *et al* 2005 Zonal flows in plasma-a review *Plasma Phys. Control. Fusion* 47 R35.

[10] Biglari H. *et al* 1990 Influence of sheared poloidal rotation on edge turbulence *Phys. Fluids B: Plasma Physics* 2 1

[11] Hahm T. S., Diamond P. H. 1987 Resistive fluid turbulence in diverted tokamaks and the edge transport barrier in H-mode plasmas *Phys. Fluids* 30 133

[12] Ko W. H. *et al* 2010 KSTAR Charge Exchange Spectroscopy System IEEE Transactions on plasma science 38 996

[13] McDermott R. M. *et al* 2009 Edge radial electric field structure and its connections to H-mode confinement in Alcator C-Mod plasmas *Phys. Plasmas* 16 056103

[14] Forest C. B. *et al* 1996 Energy Transport in Tokamak Plasmas with Central Current Density Control Using Fast Waves *Phys. Rev. Lett* 77 3141

[15] Synakowski E. J. *et al* 1997 Local transport barrier formation and relaxation in reverse-shear plasmas on the Tokamak Fusion Test Reactor *Phys. Plasmas* 4 1736

[16] Wolf R. et al 2001 Performance, heating and current drive scenarios of ASDEX Upgrade advanced tokamak discharges *Nucl. Fusion* 41 1259

[17] Schmitz L. *et al* 2012 Predator-prey oscillations and zonal flow-induced turbulence suppression preceding the L-H transition *Phys. Rev. Lett.* 108 155002

[18] Miki K. *et al* 2012 Spatio-temporal evolution of the L→I→H transition *Phys. Plasmas* 19 092306

[19] Hahm T. S. *et al* 1999 Shearing rate of time-dependent E × B flow *Phys. Plasmas* 6 922

[20] Hahm T. S. *et al* 1998 Effects of E_r/RB_θ profiles on transport reduction in DIII-D and TFTR *Plasma Phys. Control. Fusion* 40 657

[21] Sidikman K. L. *et al.*,1994 Theory of electric-field curvature effects on longwavelength drift wave turbulence *Phys. Plasmas* 1 1142

[22] Lao L. L. *et al* 1985 Reconstruction of current profile parameters and plasma shapes in tokamaks *Nucl. Fusion* 25 1611

[23] Kim Y. B. *et al* 1991 Neoclassical poloidal and toroidal rotation in tokamaks *Phys. Fluids* B 3 2050.

[24] Hirshman S. P., Sigmar D. J. 1981 Neoclassical transport of impurities in tokamak plasmas *Nucl. Fusion* 21 1079

[25] Fedorczak N. *et al* 2012 Shear-induced Reynolds stress at the edge of L-mode tokamak plasmas *Nucl. Fusion* 52 103013

[26] Kalupin D. *et al* 2005 Predictive modeling of L and H confinement modes and edge pedestal characteristics *Nucl. Fusion* 45 468

[27] Greenwald M. *et al* 2007 Density profile peaking in low collisionality H-modes: comparison of Alcator C-Mod data to ASDEX Upgrade/JET scalings *Nucl. Fusion* 47 L26